Supporting Information for

Nanoscale chemical evolution of silicon negative electrodes characterized by low-loss STEM-EELS

Maxime Boniface[1,2], *Lucille Quazuguel*[3], *Julien Danet*[1,2,‖], *Dominique Guyomard*[3], *Philippe Moreau*[3,*], *and Pascale Bayle-Guillemaud*[1,2]

[1] Université Grenoble Alpes, F-38054 Grenoble, France.
[2] CEA-INAC-MEM, F-38054 Grenoble, France.
[3] Institut des Matériaux Jean Rouxel (IMN), Université de Nantes, CNRS, 2 rue de la Houssinière, BP 32229, 44322 Nantes Cedex 3, France

*Corresponding author: philippe.moreau@cnrs-imn.fr

‖Present address: LCTS, CNRS, University of Bordeaux, Herakles-Safran, CEA, 3 Allee de La Boetie, F-33600 Pessac, France

1. Morphology of individual phases revealed through MLLS mapping.

As described in the main text, individual phase components are calculated through the MLLS routine and these can be either combined in composite color maps or presented independently. This allows for a more accurate depiction of the each phase morphology and distribution than with overlapping colors.

The fitting process itself is robust even for thick samples, although in extremely thick areas the SEI signal can be drowned out in the silicon or alloy spectrum. We are nonetheless sure that a reliable assessment of each phase morphology can be reached, particularly from observations made at the edge of the particles.

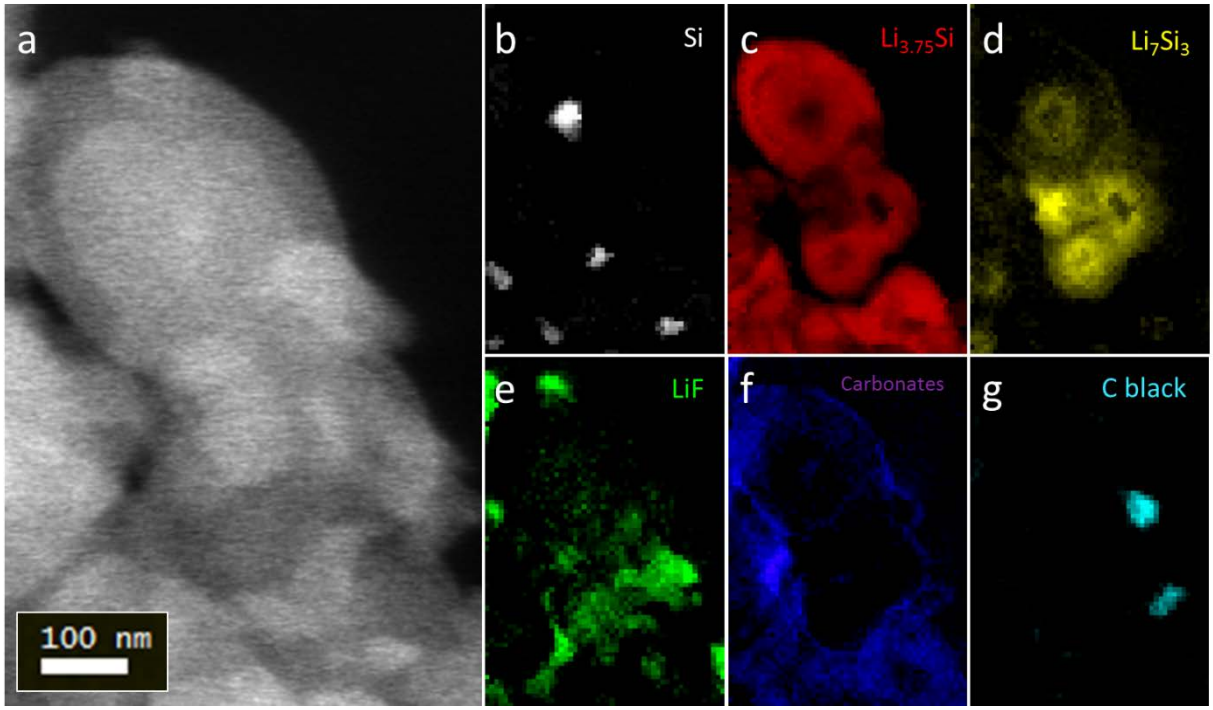

Figure S1: a) ADF-STEM image of a SiNPs aggregate after a single lithiation to 3000mAh.g^{-1}. (b-g) Individual components obtained from the MLLS fitting routine. The morphology of each phase appears clearly, especially regarding the sporadic LiF coverage and the more conformal carbonate coating. In extremely thick areas (>200nm) it is however possible that SEI signals are too weak to be decomposed properly, hence the "hollow" aspect of the carbonate component.

2. Examples of radiolysis and sputtering damage under prolonged exposure to the electron beam.

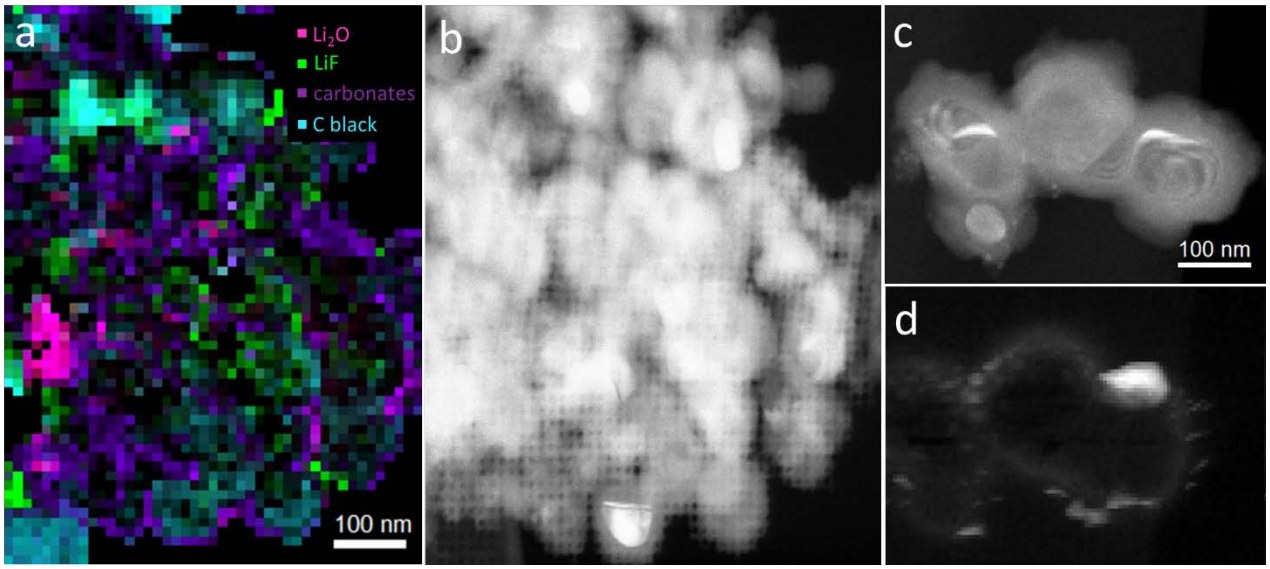

Figure S2: Examples of beam damage resulting from radiolysis in the SEI and knock-on damage in Li_xSi alloys. (a) Compound mapping of LiF (green), carbonates (purple), Li_2O (magenta) and carbon black (teal) from low-loss STEM-EELS measurements. (b) STEM image of lithiated nanoparticles and SEI after radiolysis damage resulting from overexposure to the electron beam. Mass loss can be clearly seen at discrete positions. (c) STEM image of lithiated nanoparticles before the EEL spectrum image acquisition (d) Energy-filtered image of the same area as c) at 7.5eV (corresponding to metallic Lithium) after overexposure to the electron beam. A bright area appears resulting from the sputtered Li coming from the surrounding damaged alloys.

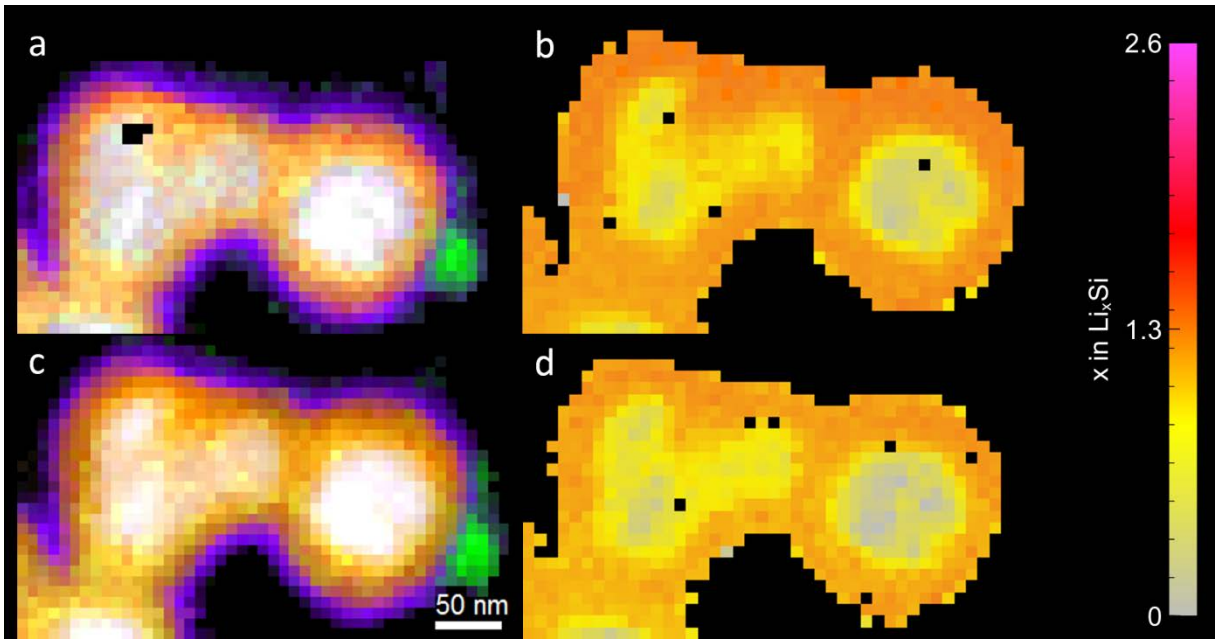

Figure S3: Examples of minimal degradation with an optimized acquisition protocol. (a-b) Successive mappings of LiF (green), carbonates (purple), silicon (white) and $Li_{2.5}Si$ (orange). (c-d) Successive mappings of x in Li_xSi showing only minimal changes.

3. Lithium content in lithium-silicon alloys quantification

Reference alloys were synthesized in the glovebox by introducing metallic lithium (Sigma Aldrich, 99.9%) and silicon nanopowder with the adequate stoichiometry to a reactor, which is then heated to 550°C for 200h. The results of the EELS analysis of these samples were plotted alongside those of Julien Danet's 2010 publication (1) and each dataset can be fitted by a quadratic function.

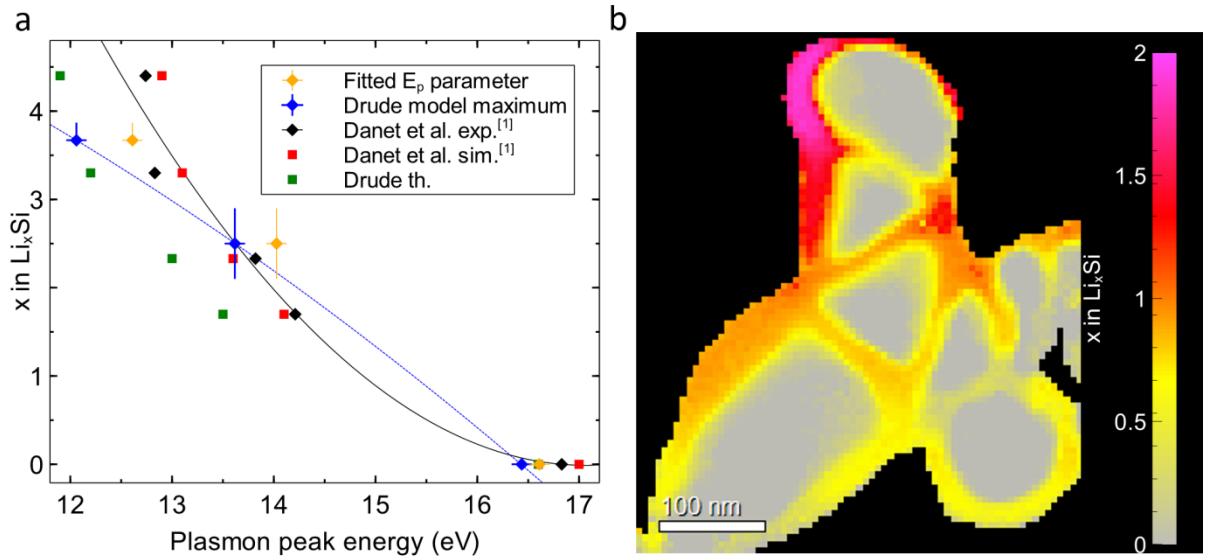

Figure S4: (a) Quantification model from the extrapolation of the experimental and simulated plasmon energies of reference alloys with known stoichiometry. (b) Example of a quantitative Li_xSi mapping on lithiated SiNPs from an electrode at its 10^{th} lithiation.

4. Delithiated particles in charged electrodes & lithium trapped in discharged electrodes

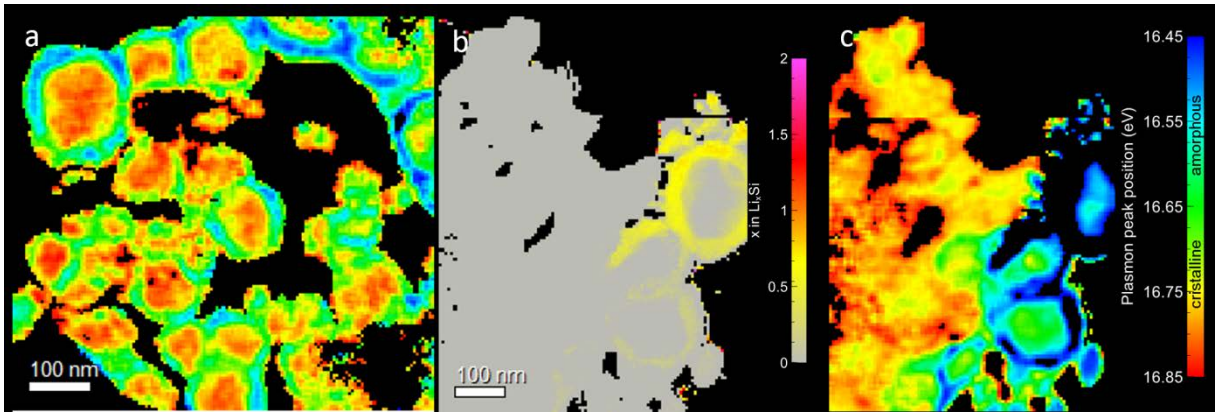

Figure S4: (a) Silicon plasmon energy mapping of a SiNP aggregate from an electrode at its 10th lithiation showing formerly active particles. (b) Li_xSi map showing a lithiated particle even after the 100th delithiation. (c) Silicon plasmon energy map showing pristine, crystalline nanoparticles even after the 100th delithiation.

(1) Danet, J.; Brousse, T.; Rasim, K.; Guyomard, D.; Moreau, P. *Phys. Chem. Chem. Phys.* **2010**, *12* (1), 220–226